Geophys. J. Int. (2006) **166,** 574–578 doi: 10.1111/j.1365-246X.2006.03068.x

FAST TRACK PAPER

Characteristic frequencies of seismic attenuation due to wave-induced fluid flow in fractured porous media

Miroslav Brajanovski,[1] Tobias M. Müller[1] and Boris Gurevich[2]

[1] *Geophysikalisches Institut, Universität Karlsruhe, Germany. E-mail: tobias.mueller@gpi.uni-karlsruhe.de*
[2] *Department of Exploration Geophysics, Curtin University & CSIRO Petroleum, Perth, Australia*

Accepted 2006 May 11. Received 2006 May 11; in original form 2005 December 7

SUMMARY

We analyse compressional wave attenuation in fluid saturated porous material with porous inclusions having different compressibilities and very different spatial scales in comparison with the background. Such a medium exhibits significant attenuation due to wave-induced fluid flow across the interface between inclusion and background. For the representative element containing two layers (one of them representing inclusion), we show that overall wave attenuation is governed by the superposition of two coupled fluid-diffusion processes. Associated with two characteristic spatial scales, we compute two cross-over frequencies that separate three different frequency regimes. At low frequencies inverse quality factor scales with the first power of frequency ω, while at high frequencies the attenuation is proportional to $\omega^{-1/2}$. In the intermediate range of frequencies inverse quality factor scales with $\omega^{1/2}$. These characteristic frequency regimes can be observed in all theoretical models of wave-induced attenuation, but quantitative estimates of their locations have been lacking so far. The potential application of this model is in estimation of the background permeability as well as inclusion scale (thickness) by identifying these frequencies from attenuation measurements.

Key words: attenuation, Biot's slow wave, diffusion, porous media, wave-induced fluid flow.

1 INTRODUCTION

One of the main intrinsic seismic wave dissipation mechanisms is associated with the wave-induced flow of the pore fluid. This effect occurs in a heterogeneous porous medium when a passing wave induces a local pore pressure gradient on the interface between inclusion and the background. In order to equilibrate pressure, viscous fluid moves across the interface. In geologically realistic structures the contrast of length scales and elastic properties between inclusions and background material might be very large. One such scenario occurs in fluid-saturated porous rocks having heterogeneous pore structure, possibly including fractures (Pride & Berryman 2003; Pride *et al.* 2004; Brajanovski *et al.* 2005).

In all these studies similar general behaviour of attenuation versus frequency is observed. In particular, for high contrast in permeabilities, compressibilities and spatial scales between inclusion and background, three different frequency regimes can be identified. Dimensionless attenuation (inverse quality factor) proportional to the first power of frequency ω at low frequencies, to $\omega^{-1/2}$ at high frequencies, and to $\omega^{1/2}$ in the intermediate frequency range, see Fig. 1. This kind of behaviour of attenuation is shown in all theoretical models of wave-induced attenuation. It is known that dissipation of energy due to a pure diffusion process is proportional to the first power of ω in the low-frequency limit and to $\omega^{-1/2}$ in the high-frequency limit (Landau & Lifshitz 1987), however, the physical description how the induced diffusional fluid motion produces intermediate frequency range, remains unclear.

In this paper we show that the intermediate frequency regime is a general feature of saturated porous media with two very distinct elastic properties of the inclusion and the background and two very different characteristic length scales that are (1) thickness of the inclusions and (2) distance between them. Based on the dispersion equation for the effective *P*-wave modulus developed by Brajanovski *et al.* (2005) for porous fractured rocks, we compute two cross-over frequencies that separate three different frequency regimes characteristic for wave-induced fluid flow attenuation in the representative element containing two layers (one of them representing inclusion). In order to give physical explanation for the intermediate $\omega^{1/2}$ frequency dependency, we show that overall wave attenuation is governed by two coupled fluid-diffusion processes, one taking place in the background and other one in the inclusion (fracture).

2 ATTENUATION OF *P*-WAVE IN FRACTURED ROCK

Brajanovski *et al.* (2005) showed that effective frequency-dependent, fluid-saturated *P*-wave modulus $c_{33}^{\rm sat}(\omega)$ of porous rock with periodic system of fractures parallel to x_1x_2 plane with spatial

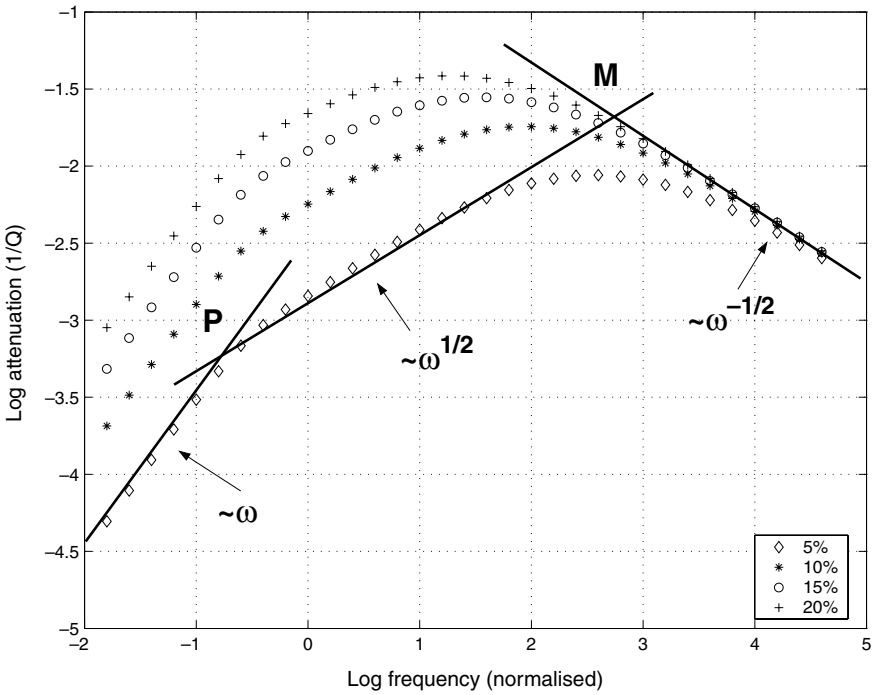

Figure 1. Log–log plot of attenuation versus circular frequency for water saturated quartz grained sandstone ($K_g = 37$ GPa, $\mu_g = 44$ GPa, $\rho_g = 2.65$ g cm^{-3}) of porosity $\phi = 0.2$ and fracture weakness Δ_N in range from 0.05 up to 0.2. Three different asymptotic parts of the attenuation curves are observed.

period H is given by

$$\frac{1}{c_{33}^{\rm sat}} = \frac{1}{C_b} + \frac{\Delta_N \left(R_b - 1\right)^2}{L_b\left[1 - \Delta_N + \Delta_N \sqrt{\mathrm{i}\Omega}\cot\left(\frac{C_b}{M_b}\sqrt{\mathrm{i}\Omega}\right)\right]}, \tag{1}$$

where Δ_N is the fracture weakness of value between 0 and 1 (Hsu & Schoenberg 1993; Bakulin *et al.* 2000), defined by $\Delta_N = Z_N L_b/(1 + Z_N L_b)$. $Z_N = \lim_{h_c \to 0}(h_c/L_c)$ is the normal excess compliance describing fracture contribution in compliance matrix in the linear-slip deformation theory (Schoenberg & Douma 1988). Index c denotes fracture parameters while index b denotes parameters of the porous background. In eq. (1) Ω is the normalized frequency given by

$$\Omega = \omega \left(\frac{H M_b}{2 C_b D_b}\right)^2. \tag{2}$$

Eq. (1) was derived in the limit $h_c/L_c \to 0$ from the more general results (Brajanovski *et al.* 2005) for a periodically stratified medium, namely a system of alternating, relatively thick layers (thickness fraction $h_b \to 1$) of a finite-porosity background material and relatively soft and thin layers (thickness fraction $h_c \to 0$) of a high-porosity material composing the open fractures. We note that the periodicity assumption is mathematically necessary, however, eq. (1) can be also used for certain random configurations as discussed in Section 5. The background material is specified by fluid-saturated P-wave velocity modulus $C_b = L_b + \alpha_b^2 M_b$, diffusivity $D_b = \kappa_b M_b L_b/\eta C_b$, permeability κ_b, pore space modulus M_b (which is practically confined bulk modulus of the pore fluid, e.g. it is the pressure to be exerted on fluid to increase relative fluid content for unity at iso-volumetric strain of matrix), dry (drained) P-wave modulus L_b and Biot–Willis coefficient α_b (describing elastic quality of the grain contacts). Viscosity of the fluid is η.

The material parameter $R_b = \alpha_b M_b/C_b$ is a coefficient of proportionality between induced pore pressure and loading total stress caused by the incident wave (Norris 1993). It contains bulk moduli of the fluid, grains and drained matrix (skeleton), respectively, porosity and P-wave velocity modulus of the drained matrix. No special assumption of shear modulus is needed because we analyse only attenuation of the compressional wave, propagating normally to the fracturing and we use fracture parametrization through the fracture weakness and normal excess compliance. The controlling parameter for induced pore pressure gradient across the fracture-background interface is the P-wave velocity modulus of drained matrix, where the shear modulus is hidden together with the bulk modulus.

Expression (1) is valid for frequencies much smaller than Biot's characteristic frequency $\omega_B = \eta\phi/\kappa\rho_f$ (fluid flow in the pore channels is Poiseuille flow), and also much smaller than the resonant frequency of the layering $\omega_R = V_p/H$ (effective medium approximation is valid), where ϕ is porosity of background, ρ_f is density of fluid and V_p is velocity of P-wave. Within the condition $\omega \ll \min(\omega_B, \omega_R)$, we can still define low and high frequencies with respect to fluid flow. Low frequencies are those when pressure has enough time to equilibrate between layers during the half-period of wave, while for high frequencies this is not possible.

The resulting medium is anisotropic, furthermore, anisotropy is frequency dependent. Brajanovski *et al.* (2005) derived effective limiting low- and high-frequency elements of the stiffness tensor for such a medium.

From eq. (1) we compute complex P-wave velocity $V_{p3} = \sqrt{c_{33}^{\rm sat}/\rho_b}$, where $\rho_b = \rho_g(1 - \phi_b) + \rho_f\phi_b$ is mass density of the fluid-saturated background material. The P-wave phase velocity is $V_p = [\mathrm{Re}\,(V_{p3}^{-1})]^{-1}$ and the attenuation Q^{-1} is given by $Q^{-1} = 2V_p \mathrm{Im}(V_{p3}^{-1})$. The results of Q^{-1} as a function of frequency for different values Δ_N are computed for a typical reservoir rock. In Fig. 1, where $\log\,(Q^{-1})$ is plotted versus $\log\omega$, we observe that the normalized frequency for peak attenuation decreases with increasing fracture weakness Δ_N. In the high-frequency limit the attenuation is

proportional to $\omega^{-1/2}$. In the low-frequency limit attenuation is proportional to ω. From the curve marked with diamonds, for the case of lower fracture weakness (which intuitively corresponds to 'thinner' fractures), we clearly observe a transitional part proportional to $\omega^{1/2}$. Points P and M define cross-over frequencies separating attenuation behaviour into frequency regimes whose asymptotes are given by ω to the power of 1, 1/2 and $-1/2$, respectively. In the next section we derive analytical expressions for these cross-over frequencies and investigate their dependence on fracture parameters. This analysis is followed by a qualitative interpretation of a coupled diffusion process leading also to estimates of the cross-over frequencies (Section 4). Thus, readers who are not interested in the technicalities may continue with Section 4.

3 ASYMPTOTIC ANALYSIS AND CHARACTERISTIC FREQUENCIES

A direct calculation of the cross-over frequencies from eq. (1) is not feasible. Therefore, a simpler but approximate recipe is used: estimates of the two cross-over frequencies can be obtained from the intersection points of the three asymptotes. From the definition of Q^{-1} and dispersion relation (1) we find an asymptotic solution for imaginary parts of the complex velocity V_{p3} normalized by the constant real velocity $\sqrt{C_b/\rho_b}$. Therefore, in order to compute low-frequency asymptote we only need to consider the expression

$$\mathrm{Im}\frac{1}{c_{33}^{\mathrm{sat}}} = \mathrm{Im}\left\{T\left[\frac{1}{\Delta_N} - 1 + \sqrt{i\Omega}\cot\left(\frac{C_b}{M_b}\sqrt{i\Omega}\right)\right]^{-1}\right\}, \tag{3}$$

where $T = L_b^{-1}(R_b - 1)^2$. Eq. (3) can be simplified by using the expansion of $\cot z$ for small argument z

$$\mathrm{Im}\left\{T\left[\left(\frac{1}{\Delta_N} - 1 + \frac{M_b}{C_b}\right) - i\frac{\Omega C_b}{3M_b}\right]^{-1}\right\} \approx \frac{T\Omega C_b}{3M_b B^2}, \tag{4}$$

where $B = (1/\Delta_N + M_b/C_b - 1)$. Hence, Q^{-1} is proportional to Ω or ω.

To find the intermediate asymptote we apply the following procedure. From eq. (1) and also Fig. 1 we deduce that this intermediate attenuation regime becomes broader for smaller fracture weakness. That means we have to analyse the double limit, first take the approximation for small fracture weakness and then take the limit as frequency goes to zero. Small Δ_N limit is obtained from eq. (1) using

$$\begin{aligned}\mathrm{Im}\frac{1}{c_{33}^{\mathrm{sat}}} &= \mathrm{Im}\frac{T\Delta_N}{1 - \Delta_N + \Delta_N F}\\ &\approx \mathrm{Im}T\Delta_N(1 + \Delta_N - \Delta_N F) = T\Delta_N^2\mathrm{Im}F,\end{aligned} \tag{5}$$

where $F = \sqrt{i\Omega}\cot(C_b\sqrt{i\Omega}/M_b)$. The low-frequency limit requires only analysis of ImF. We calculate ImF by representing cotangent function of complex argument in exponential form and then expressing the result in terms of trigonometric and hyperbolic functions

$$\begin{aligned}\mathrm{Im}F &= \mathrm{Im}\; i\sqrt{i\Omega}\frac{\exp\left[i\frac{C_b}{M_b}\sqrt{i\Omega}\right] + \exp\left[-i\frac{C_b}{M_b}\sqrt{i\Omega}\right]}{\exp\left[i\frac{C_b}{M_b}\sqrt{i\Omega}\right] - \exp\left[-i\frac{C_b}{M_b}\sqrt{i\Omega}\right]}\\ &= \mathrm{Im}\;(i-1)\frac{\sqrt{\Omega}}{\sqrt{2}}\frac{(\cos P\cosh P - i\sin P\sinh P)^2}{\cos^2 P\cosh^2 P + \sin^2 P\sinh^2 P},\end{aligned} \tag{6}$$

or

$$\begin{aligned}\mathrm{Im}F = \frac{\sqrt{\Omega}}{2(\cos^2 P\cosh^2 P + \sin^2 P\sinh^2 P)}&\\ \times(\cos^2 P\cosh^2 P - \sin^2 P\sinh^2 P&\\ + 2\cos P\cosh P\sin P\sinh P)&\end{aligned} \tag{7}$$

where $P = C_b\sqrt{\Omega}/(\sqrt{2}M_b)$. As $\Omega \to 0$ and $P \to 0$, the expansion of eq. (7) gives

$$\mathrm{Im}F = \frac{\sqrt{\Omega}}{2}(1 + \mathcal{O}(P^2)). \tag{8}$$

Substitution of ImF into eq. (5) yields

$$\mathrm{Im}\frac{1}{c_{33}^{\mathrm{sat}}} = \frac{T\sqrt{\Omega}\Delta_N^2}{2}. \tag{9}$$

The latter equation shows that in the double limit of small fracture weakness and low-frequency Q^{-1} is proportional to $\omega^{1/2}$; Fig. 1 clearly demonstrates this dependency.

The lower cross-over frequency can be computed by looking at intersection of these two asymptotes. Equating right-hand sides of eqs (4) and (9), and substituting $B \approx 1/\Delta_N$ gives normalized cross-over frequency Ω_P for point P

$$\Omega_P = \left(\frac{3M_b}{2C_b}\right)^2. \tag{10}$$

From eq. (2) we calculate the corresponding real angular frequency ω_P

$$\omega_P = 9\frac{D_b}{H^2}. \tag{11}$$

The high-frequency asymptote can be obtained in a similar way. Writing the cotangent function in exponential form and taking limit $\Omega \to \infty$ and $P \to \infty$, we get imaginary part of the modulus

$$\mathrm{Im}\frac{1}{c_{33}^{\mathrm{sat}}} = \mathrm{Im}\frac{T}{\frac{1}{\Delta_N} - 1 - \frac{i-1}{\sqrt{2}}\sqrt{\Omega}} \approx \frac{T}{\sqrt{2\Omega}}, \tag{12}$$

thus, for high frequencies Q^{-1} is proportional to $\omega^{-1/2}$.

Equating right-hand sides of eqs (9) and (12) gives the upper normalized cross-over frequency Ω_M (point M), which is an approximation for the maximum of attenuation

$$\Omega_M = \frac{\sqrt{2}}{\Delta_N^2}. \tag{13}$$

From eq. (2), the corresponding real angular frequency ω_M is

$$\omega_M = 4\sqrt{2}\left(\frac{C_b}{M_b}\right)^2\Delta_N^{-2}\frac{D_b}{H^2}. \tag{14}$$

Substituting Ω_M from the eq. (13) into eq. (1), shows that the peak attenuation is proportional to Δ_N: $\quad Q_M^{-1} = 2^{-3/4}\,\Delta_N$.

The main results of this section are the estimates of the cross-over frequencies, eqs (11) and (14). In the next section we provide a physical explanation of their dependence on poroelastic parameters and on the length scales involved.

4 INTERPRETATION OF THE COUPLED DIFFUSION PROCESS

We will now show that for the periodic system consisting of two layers with different compliances and different thicknesses (for example, thin fractures embedded in a porous background rock) under compressional loading the attenuation behaviour described in

the previous section can be interpreted as a superposition of two coupled diffusion processes. Although, each layer alone does not produce any attenuation (layer itself is homogeneous), when connected together, attenuation takes place because the pore pressure gradient across the interface is induced. In order to equilibrate pressure, fluid flow occurs between layers (background and fracture). This process is described by the diffusion equation. Symmetry of the system causes no-flow condition in the middle of each layer (White *et al.* 1975). One can say that condition for the maximal attenuation is when fluid penetrates layer to the maximal possible depth. Therefore, the condition of *diffusion resonance* for each layer is given by (a) the equality of diffusion length $\delta_{b,c} = \sqrt{2D_{b,c}/\omega}$ in particular layer and half-thickness of the layer and by (b) the hydraulic coupling as a consequence of fluid mass conservation. We use the word *resonance* by analogy with waves because the pore pressure diffusion processes under consideration can be also interpreted in terms of Biot's slow compressional wave (Chandler & Johnson 1981). In that sense the total attenuation is a result of the interference of Biot's slow waves in each layer.

Let us interpret how pore pressure diffusion process behaves in the background rock. The cross-over frequency ω_P(11) is independent of fracture weakness Δ_N and depends merely on the ratio between diffusivity and thickness of the background layer. This is understandable since the diffusion length δ_c in the fracture at low frequencies is several orders of magnitude bigger than the fracture thickness; such that it has only negligible impact on the frequency dependency of the diffusion process in the background. If it was possible for a diffusion process in the background to exist alone then its resonant frequency would be defined by the equality of the diffusion length and the half-thickness so that

$$\omega_{P'} = 8\frac{D_b}{H^2}. \tag{15}$$

This estimate is very close to the cross-over frequency given by eq. (11).

We note that in eq. (14) for upper cross-over frequency ω_M there is no explicit dependency of the fracture diffusivity. The reason is that in eq. (1) fracture properties are lumped into a single parameter that is fracture weakness. Underlying physical reason is the high contrast in spatial scales and compressibilities, which allows simpler parametrization of fractures (Schoenberg & Douma 1988; Bakulin *et al.* 2000) via fracture weakness parameter. Let us see how fracture thickness affects the upper cross-over frequency ω_M. By using the definition of fracture weakness, the 'softness' of the thin layer can be expressed through the parameter

$$\frac{1}{Z_N} = \frac{L_b\,(1-\Delta_N)}{\Delta_N}, \tag{16}$$

then, $L_c = h_c/Z_N$, showing that dry modulus of fracture skeleton $L_c \to 0$, as $h_c \to 0$. Substituting Δ_N from eq. (16) for small Δ_N gives

$$\frac{1}{Z_N} = \frac{L_c}{h_c} \approx \frac{L_b}{\Delta_N}, \tag{17}$$

and for upper cross-over frequency from eq. (14) we get

$$\omega_M = 4\sqrt{2}\frac{D_b}{N_b^2}\left(\frac{L_c}{h_c H}\right)^2, \tag{18}$$

where $N_b = D_b\eta/\kappa$ is a poroelastic modulus, $H \approx h_b H$ is the fracture distance and $h = h_c H$ is the fracture thickness. For weakly consolidated fracture matrix Gassmann equation yields $C_c \approx M_c$, so $L_c \approx N_c$ and from eq. (18) we get

$$\omega_M = 4\sqrt{2}\left(\frac{N_c}{N_b}\right)^2\frac{D_b}{h^2}. \tag{19}$$

The cross-over frequency ω_M primarily depends on fracture thickness (weakness). Since diffusion length in the background is smaller than the diffusion length in open fracture the coupling of the two diffusion processes is strong (amount of fluid that can flow across the interface is influenced by D_b). Then from eq. (19) we deduce an *effective* fracture diffusivity $D_c \propto (N_c/N_b)^2\,D_b$.

In conclusion, the coupled diffusion process with its characteristic frequencies ω_P and ω_M can be interpreted as a superposition of two partial diffusion processes. Each partial diffusion process has a characteristic frequency, which is proportional to the ratio of diffusivity and square of the characteristic length scale (eqs 15 and 19). From eqs (11) or (15) and (19) we find relation

$$\frac{\omega_M}{\omega_P} \propto \left(\frac{N_c}{N_b}\right)^2\left(\frac{H}{h}\right)^2, \tag{20}$$

confirming that separation of cross-over frequencies depends on the ratios of spatial scales and poroelastic moduli. Identification of these cross-over frequencies provides a mean to estimate transport properties as discussed in the next section.

5 DISCUSSION AND CONCLUSION

In the layered porous medium with similar thicknesses of layers, both diffusivities affect the cross-over frequencies ω_P and ω_M. A total maximum is created as a result of superposition. Intermediate frequency regime of attenuation is hardly visible because ω_P and ω_M are close to each other. What happens when one of the layers is several orders of magnitudes thinner and softer than the other? The characteristic frequencies evaluated in previous sections provide an answer in terms of relevant material properties. In particular, from eqs (11), (14) and (20) we conclude that separation between ω_P and ω_M becomes stronger for smaller fracture weakness (smaller fracture thickness) and stiffer background matrix (or softer fracture matrix).

The results derived from eq. (1) are limited by the assumption of periodic distribution of fractures. In reality fractures may be distributed in a random fashion. Sensitivity of our results to the violation of the periodicity assumption was examined numerically using reflectivity modelling for layered poroelastic media (Lambert *et al.* 2006). Numerical experiments for a random distribution of fractures of the same thickness still show good agreement with theoretical results obtained for periodic fractures in a vicinity of the attenuation peak. However the regime with Q^{-1} proportional to ω is no longer present, and the 'intermediate' frequency range with $Q^{-1} \propto \omega^{1/2}$ extends over the low-frequency range. This numerical result for a random distribution of fractures is in agreement with both theoretical and numerical results for randomly layered porous media with small contrast between layers (Gurevich & Lopatnikov 1985; Gelinsky *et al.* 1998).

We think that these results represent a general feature of attenuation due to the so-called mesoscopic flow (in the presence of heterogeneities small compared to the wavelength but much larger than the size of individual pores or grains) in double-porosity structures. In fact, the three different frequency regimes identified here can be clearly observed in the attenuation behaviour of double-porosity configurations as shown in Pride *et al.* (2004) (see their Fig. 1). Similar intermediate frequency regime is observed in patchy-saturation

model (Johnson 2001) however, magnitude of attenuation is much smaller because the overall elastic rock properties do not exhibit big contrast, and thus if the spatial scales of fluid patches are very different the overall effect of small heterogeneities is small. According to Norris (1993): 'The general mechanism does not assume partial saturation, but only that the medium is inhomogeneous. For example, the pores could be completely saturated with liquid but the compressibility of the solid frame may vary with position. However, the diffusion is greater if the fluid compressibility varies significantly from point to point', so the similarity of attenuation frequency dependency in different scenarios is expected.

Since natural fractures control the permeability of the reservoir, the ability to find and characterize fractured areas of the reservoir represents a major challenge for seismic investigations. Up-to-date methodology for fracture weakness estimation from surface seismic data is based on Thomsen-style anisotropic coefficients (Bakulin *et al.* 2000). We note that the fracture weakness Δ_N is introduced for a purely *elastic* fractured medium. However, from measurements we estimate a *poroelastic* fracture weakness, which possibly includes hydraulic interaction between fractures and pores of the background rock (squirt-flow type mechanism). As a consequence, the estimated fracture weakness can lead to non-unique information about fracture filling, except in the case of isolated fluid-filled fractures or dry ones (Bakulin *et al.* 2000). The frequency-dependent attenuation may provide additional constraints on fracture weakness estimation.

The presented results give a physical basis for estimation of the reservoir permeability. These parameters may provide additional input for reservoir modelling. The major requirement for such an approach is that measurements must be made over a relatively broad frequency range (between seismic and sonic logging frequencies). The principal difficulty lies in the fact that each of the seismic and acoustic technologies—reflection seismology, sonic logging, ultrasonic measurements—cover a relatively narrow frequency band. Interpretation of narrow band attenuation measurements is ambiguous, as attenuation may be caused by other mechanisms, such as scattering. We think that analysis of data from cross-hole measurements, often using an input sweep signals in range 200–4000 Hz, enables us to reconstruct intermediate parts of the dispersion and attenuation curves using or developing procedures for processing of transient signals. Another possible source of multi-frequency data is special logging tool that operates in frequency range 500–5000 Hz. *P*-wave velocities in the low- and high-frequency limit can be estimated from VSP and sonic log data, respectively. By fitting the theoretical model to the real data we can estimate the parameters of both the fractures and background rock. The characteristic frequencies yield estimates of permeabilities and thicknesses of the background-fractures system. The results of this study establish the physical principles for the development of such a methodology.

ACKNOWLEDGMENTS

The instructive comments and suggestions of the two reviewers helped to improve the quality of the manuscript. This work was kindly supported by the Deutsche Forschungsgemeinschaft (contract MU 1725/2-1).

REFERENCES

Bakulin, A., Grechka, V. & Tsvankin, I., 2000. Estimation of fracture parameters from reflection seismic data—part I: HTI model due to a single fracture set, *Geophysics,* **65,** 1788–1802.

Brajanovski, M., Gurevich, B. & Schoenberg, M., 2005. A model for *P*-wave attenuation and dispersion in a porous medium permeated by aligned fractures, *Geophys. J. Int.,* **163,** 372–384, doi:10.1111/j.1365–246X.2005.02722.x.

Chandler, R.N. & Johnson, D.L., 1981. The equivalence of quasistatic flow in fluid-saturated porous media and Biot's slow wave in the limit of zero frequency, *J. Appl. Phys.,* **52,** 3391–3395.

Gelinsky, S., Shapiro, S., Müller, T. & Gurevich, B., 1998. Dynamic poroelasticity of thinly layered structures, *Internat. J. Solids Structures.,* **35,** 4739–4752.

Gurevich, B. & Lopatnikov, S.L., 1985. Attenuation of longitudinal waves in a saturated porous medium with random inhomogeneities, *Doklady Earth Science Sections,* **281,** 47–50.

Hsu, C. & Schoenberg, M., 1993. Elastic waves through a simulated fractured medium, *Geophysics,* **58,** 964–977.

Johnson, D.L., 2001. Theory of frequency dependent acoustics in patchy-saturated porous media, *J. acoust. Soc. Am.,* **110,** 682–694.

Lambert, G., Gurevich, B. & Brajanovski, M., 2006. Attenuation and dispersion of P-waves in porous rocks with planar fractures: comparison of theory and numerical simulations, *Geophysics,* **71,** N41–N45.

Landau, L. & Lifshitz, E., 1987. *Fluid Mechanics,* Permagon, Oxford.

Norris, A.N., 1993. Low-frequency dispersion and attenuation in partially saturated rocks, *J. acoust. Soc. Am.,* **94,** 359–370.

Pride, S.R. & Berryman, J.G., 2003. Linear dynamics of double-porosity dual-permeability materials, 1. Governing equations and acoustic attenuation, *Physical Review E.,* **68,** 036603.

Pride, S., Berryman, J.G. & Harris, J.M., 2004. Seismic attenuation due to wave-induced flow, *J. geophys. Res.,* **109**(B1), B01201.

Schoenberg, M. & Douma, J., 1988. Elastic-wave propagation in media with parallel fractures and aligned cracks, *Geophys. Prospect.,* **36,** 571–590.

White, J.E., Mikhaylova, N.G. & Lyakhovitsky, F.M., 1975. Low-frequency seismic waves in fluid saturated layered rocks, *Izvestija Academy of Sciences USSR, Phys. Solid Earth,* **11**(10), 654–659.